Critical Reynolds Number for Sinusoidal Flow of Water in Rigid Tubes

DANIEL HERSHEY and CHI SOON IM

University of Cincinnati, Cincinnati, Ohio

In steady flow at Reynolds number above 2,100, many investigators have proposed that laminar flow is usually unstable and a disturbance will probably be magnified, eddies will form and the laminar flow will break up into partially developed turbulent flow. In special circumstances, including cases where the flow at the tube entrance is particularly disturbed, some investigators, Sorkau (*20*), Carothers (*1*), and Grindley and Gibson (*8*) have found that the viscous laminar range extends only over a range of Reynolds number from 200 to 400. Usually flow data for laminar flow, the transition region, and turbulent flow are displayed on a logarithmic plot of the Fanning friction factor,

$$f = \frac{(\Delta p)_{avg}(R)\, g_c}{\langle u \rangle^2 L} \tag{1}$$

versus the Reynolds number,

$$N_{Re} = \frac{2R\langle u \rangle}{\nu} \tag{2}$$

Since Von Kries (*22*) published a pioneering theory of pulsatile flow that is most applicable to large vessel flows, many experimental as well as theoretical investigations on pulsatile flow have been made (*2, 13, 19, 21, 25*). The conditions under which laminar or turbulent flow can exist in the cardiovascular system have long been of concern to physiologists (*3, 5, 9, 15, 23*). Within recent years pulsatile flow has received an increased amount of attention from engineers as well as physiologists. Darling (*4*), working with water and a 50% glycerol solution in a 0.379 in. diameter pipe found that the critical Reynolds number dropped from 2,500 in steady flow to 1,500 in pulsing flow. Kastner and Shih (*12*) measured the transition Reynolds number for pulsating flow of air between two parallel flat plates and found a decrease in the value of the critical Reynolds number. Gilbrech and Combs (*6, 7*) used water as the working fluid and determined the characteristics of turbulent plugs from photocell signal recording. Their results indicated a critical Reynolds number that was higher under some conditions of flow than the steady flow Reynolds number of 2,100. Their experimental data also indicated that the critical Reynolds number decreased as the amplitude of the pulsations was increased from zero. In Sarpkaya's work (*17*), the critical Reynolds number for pulsating flow was higher than the critical Reynolds number of the steady Poiseuille flow for the same mean pressure gradient. He observed that the critical Reynolds number decreased as the frequency parameter $\Omega = a\left(\frac{w}{\nu}\right)^{1/2}$ increased for a given value of velocity ratio. Yellin (*26, 27*) did not investigate the critical Reynolds number but determined the influence of the oscillating component of flow on the steady flow transition characteristics. Yellin also used an optical technique to measure both slug characteristics and intermittency. He also found (*26*) that the kinematics of spontaneous and artificial slugs are identical.

Recently, a theoretical relation between friction factor and Reynolds number for pulsatile Newtonian flow has been proposed by Hershey and Song (*10*). In laminar pulsatile flow, the friction factor correlation that they derived was

$$f_p = (\pi/16\ S)\ (16/N_{Re}) \tag{3}$$

which yields the standard Fanning friction factor relationship $f = 16/N_{Re}$ when the frequency factor $\lambda = R^2\Omega/\nu$ goes to zero. Equation (3) presents a method for establishing the critical Reynolds number for pulsatile flow that is analogous to the $f - N_{Re}$ method in steady flow. Thus a logarithmic plot of friction factor versus Reynolds number should yield a straight line up to the critical Reynolds number where the friction factor values should markedly increase in value.

EXPERIMENTAL EQUIPMENT & PROCEDURE

It was necessary to obtain pressure drop and flow rate data for the pulsatile flow and the corresponding steady flow before Equation (3) could be utilized for the determination of the critical Reynolds number. Schematically, the experimental flow system is shown in Figure 1. This is the same equipment used by Hershey and Song (*10*) in their work. Four different sized Pyrex glass tubes of 0.25 ot 0.8 cm. diameter and about 1 meter in length were used. Two holes drilled 75 cm. apart served as the pressure measuring taps in this study. Connected to these pressure taps were pressure transducers as shown in Figure 1, item *P*. As shown in Figure 1, a pulse generator was joined to the steady flow line to produce a sinusoidal laminar flow. The pulse was generated by a syringe (20 cc.) which was moved by a scotch yoke connected to a ⅛ horse power variable speed motor. The average flow rate was measured directly with a graduated cylinder and a stopwatch. The pressure drop was determined by pressure transducers, *P*, which were excited by power suppliers, *S*, and recorded by a dual channel recorder. In order to adjust the pressure zero point and the pressure range, a compressed air line was connected by valve *D* to *F* and a mercury manometer *M*.

Water was used in this experiment. Seven different frequencies, 10 to 70 cycles /min., were used with various amplitudes. All experiments were conducted at room temperature 25°C.

The amplitude of the syringe stroke was changed by adjusting the scotch yoke and the pressure frequency was varied by adjusting the screw-type motor speed controller. After adjusting the scotch yoke and the motor speed to desired values, a pressure pulse was generated by starting the motor which drives the scotch yoke. Complete details are given elsewhere (*11, 17*).

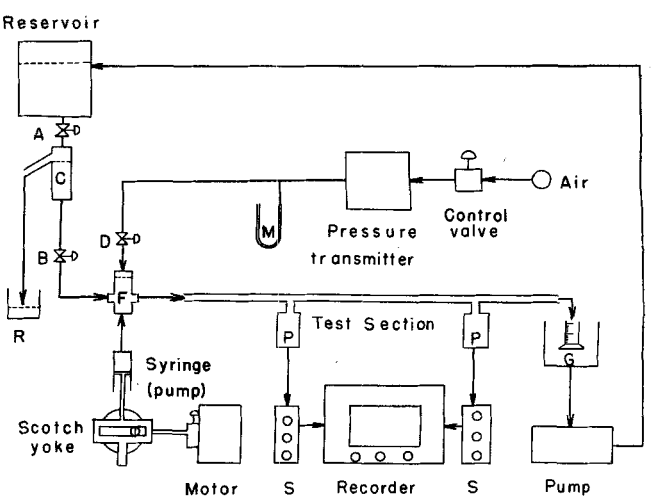

Fig. 1. The experimental flow diagram.

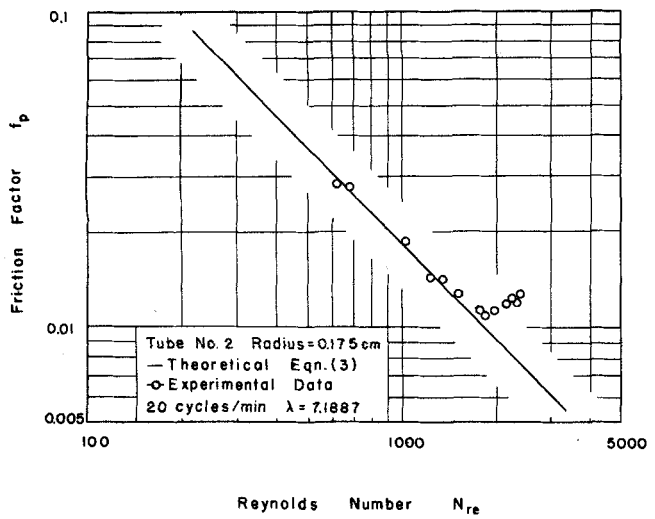

Fig. 2. Friction factor vs. Reynolds number for water.

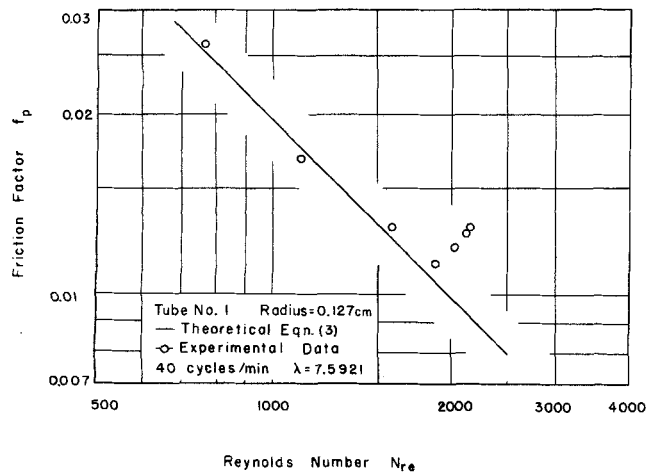

Fig. 3. Friction factor vs. Reynolds number for water.

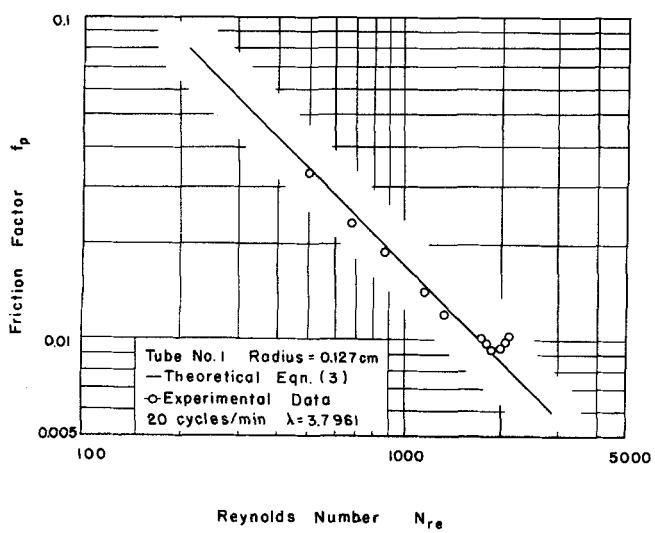

Fig. 4. Friction factor vs. Reynolds number for water.

PRESENTATION OF DATA AND RESULTS

The experimental friction factor was calculated from Equation (1) with the average pressure drop obtained from the recorder strip chart and the theoretical friction factor was calculated by using Equation (3). Figures 2, 3, 4 represent the typical results, showing clearly the departure from laminar flow for this sinusoidally pulsing flow. Figure 5 is a summary of all the experimental results, correlating the critical Reynolds number with the frequency

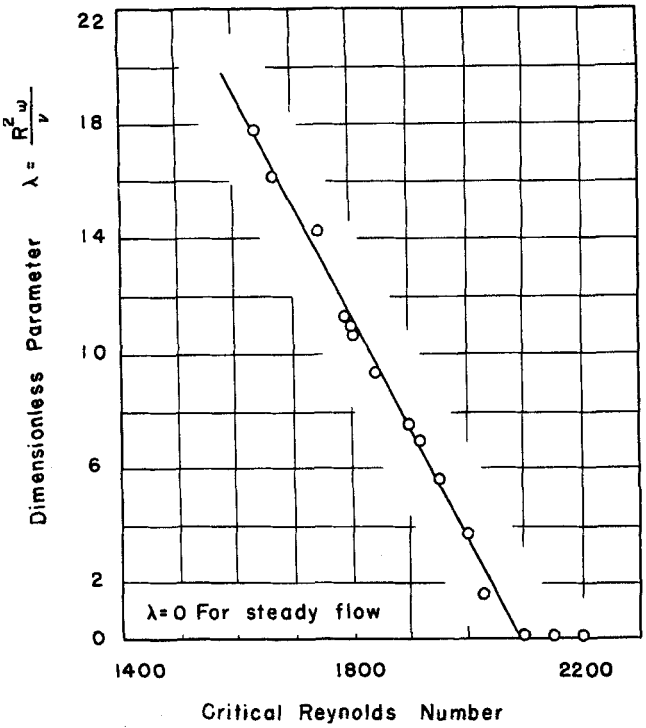

Fig. 5. Critical Reynolds number vs. dimensionless parameter $\lambda = \frac{R^2\Omega}{\nu}$.

factor, λ.

As can be seen from the figures, there is excellent agreement between theory (Hershey and Song) and experiment for laminar flow. Since Equation (3) is applicable only in pulsatile laminar flow, it would be expected that the theory would not represent the experimental data outside of the laminar regime. This deviation is interpreted as the onset of the transition from laminar to turbulent flow. From Figure 5 it is observed that the critical Reynolds number increases as λ decreases, which agrees with the results of Gilbrech and Combs (*5, 6*), and Sarpkaya (*15*).

ACKNOWLEDGMENT

This work was partially supported by National Institutes of Health Grant HE-08781 and NASA Grant NGR 36-004-014.

NOTATION

f = friction factor
g_c = 32.174 (lb.-mass) (ft.)/(lb.-force) (sq.sec.)
L = distance between pressure taps
P, P_o = pressure
$(\Delta P)_{avg}$ = average pressure drop for pulsatile flow
R = radius of tube
r = axis of radial direction

$$S = \sum_{n=1}^{\infty}\left[\frac{2\pi}{\mu_n^4} + \frac{1}{\lambda\mu_n^2 + \mu_n^6/\lambda} - \frac{\lambda}{\mu_n^6}\right](1 - e^{2\pi\nu\mu_n^6/R^2})$$

u = velocity of fluid
$<u>$ = time average velocity of fluid
z = axial direction of the tube

Greek Letters

ν = kinematic viscosity = μ/ρ
λ = dimensionless parameter defined by R^2w/ν
μ_n = roots of zero order Bessel function
μ = viscosity of fluid
ρ = density of fluid
w = angular velocity

LITERATURE CITED

1. Carothers, *Proc. Roy. Soc. (London)., Ser., A*, **87**, 154 (1912).
2. Chantry, W. A., R. L. Von Berg, and H. F. Wiegandt, *Ind. Eng. Chem.*, **47**, 1153 (June, 1955).
3. Coulter, N. A., Jr., and J. R. Pappenheimer, *Am. J. Physiol.*, **159**, 401 (1949).
4. Darling, G. B., *Petroleum*, **22**, 177 (1959).
5. Fries, E. D., and W. C. Heath, *Circulation Res.*, **14**, 105 (1964).
6. Gilbrech, D. A., and G. D. Combs, *Theoretical Applied Mech.*, **1**, 292 (1963).
7. ————, *Eng. Exp. Sta.*, Univ. Arkansas, Fayatteville, **4**, (April, 1964).
8. Grindley and Gibson, *Proc. Roy. Soc. (London)., Ser. A*, **80**, 114 (1908).
9. Helps, E. P. W., and D. A. McDonald, *J. Physiol.*, **124**, 631 (1954).
10. Hershey, D., and G. S. Song, *AIChE J.*, **13**, 491 (1967).
11. Im, C. S., M S thesis, Univ. Cincinnati, Ohio (1967).
12. Kastner, L. J. and S. H. Shih, *Engineering*, **172**, 389 (1951).
13. Linford, R. G., Ph.D. thesis, Univer. Utah, (1961).
14. McDonald, D. A., "Blood Flow in Arteries," Arnold, London (1960).
15. Ralston, J. H. and A. N. Taylor, *Am. J. Physiol.*, **144**, 706 (1945).
16. Reynolds, O., *Trans. Roy. Soc. (London), Ser. A*, **174**, 935 (1883).
17. Sarpkaya, T., *Trans. Am. Soc. Mech. Eng., no. 66-FE-5* (1966).
18. Shirotsuka, T., *Kagaku Kikai*, **21**, 638 (1957).
19. Song, G., Ph.D. thesis, Univ. Cincinnati, Ohio (1966).
20. Sorkau, Z. *Phys.*, **14**, 759 (1913).
21. Taylor, M. G., *Phy. Med. Biol.*, **1**, 258 (1957).
22. Von Kries, *Akad. Uerlagsbuch*, 8 (1892).
23. Wesolowski, S. A., C. C. Fries, A. M. Sabini, and P. N. Sawyer, "Biophysical Mechanisms in Vascular Homeostasis and Intravascular Thrombosis," P. N. Sawyer, ed., Appleton-Century-Crofts, New York (1965).
24. Womersley, J. R., *Wright Air Devel. Center, TR 56-614* (1957).
25. ———, *J. Physiol.*, **127**, 553 (1955).
26. Yellin, E. L., *Am. Soc. Mech. Eng., 66-WA/BHF-I* (1966).
27. ———, *Circulation Res.*, **19**, 791 (Oct., 1966).
28. ———, Ph.D. thesis, Univ. Illinois, Urbana (1964).

Interaction Energy in Surface Diffusion

SUN-TAK HWANG

University of Iowa, Iowa City, Iowa

The gas-solid interaction is the most important quantity in the physical adsorption of gas molecules on solids. If the surface diffusion of the adsorbed molecule is to be studied fundamentally, then it seems logical to investigate and analyze the gas-solid interaction energy for the system. There are some publications (*2, 3, 6, 7, 12, 14*) which deal with the calculation of the dispersion energy for both homogeneous and heterogeneous systems. However, no one has attempted to apply those techniques to the study of surface diffusion.

In the present paper, various correlations are presented for the gas-solid interaction energies and fundamental physical properties of the gases. These correlations were found to be very useful in predicting the amount of surface diffusion, which will occur when a gas or vapor flows through a microporous medium.

SURFACE DIFFUSION

The surface diffusion of gases and vapors through microporous media represents a significant contribution to the total transport. If the surface coverage of the adsorbed molecules is low and the Knudsen regime prevails Equation (1) will prove to be adequate over a wide temperature range to explain the flow data of many gases and vapors through microporous Vycor glass (*9* to *11*):

$$Q\sqrt{MT} = A + BT \exp(\Delta/T) \qquad (1)$$

Here A represents the Knudsen flow, which thus remains constant for a given microporous medium. The second term representing the surface flow, however, is a function of values of B and Δ which vary from gas to gas. The definition of Δ is

$$\Delta = \frac{\epsilon^s - \epsilon^t}{k} \qquad (2)$$

where ϵ^s is the gas-solid interaction energy and ϵ^t is the activation energy of surface diffusion for an adsorbed molecule. Therefore, the value of Δ is a measure of the interaction energy between the gas molecule and the solid surface. This was demonstrated in an earlier crude correlation (*9*). Since there exists an interrelationship [(*9*) also, see Figure 4 of the present paper] between B and Δ, if the value of Δ can be estimated from other physical properties, then one can easily calculate the